



HAL
open science

Thermodynamic analysis of a thermochemical storage process using a multisalt open fixed bed reactor

Benoit Michel, Lauren Farcot, Nolwenn Le Pierrès

► **To cite this version:**

Benoit Michel, Lauren Farcot, Nolwenn Le Pierrès. Thermodynamic analysis of a thermochemical storage process using a multisalt open fixed bed reactor. ECOS (Efficiency, Cost, Optimization, Simulation and environmental impact of energy systems), Jun 2016, Portoroz, Slovenia. hal-01734573

HAL Id: hal-01734573

<https://hal.science/hal-01734573>

Submitted on 14 Mar 2018

HAL is a multi-disciplinary open access archive for the deposit and dissemination of scientific research documents, whether they are published or not. The documents may come from teaching and research institutions in France or abroad, or from public or private research centers.

L'archive ouverte pluridisciplinaire **HAL**, est destinée au dépôt et à la diffusion de documents scientifiques de niveau recherche, publiés ou non, émanant des établissements d'enseignement et de recherche français ou étrangers, des laboratoires publics ou privés.

ECOS 2016:

Thermodynamic analysis of a thermochemical storage process using a multisalt open fixed bed reactor

Benoit MICHEL^{a,}, Lauren FARCOT^{a,b}, Nolwenn LE PIERRES^a*

^a *Université Savoie Mont Blanc - CNRS, LOCIE, Le Bourget-du-Lac, France*

^b *CEA/DTBH/SBRT/LSHT, Le Bourget-du-Lac, France*

* E-mail: benoit.michel@univ-smb.fr

Abstract:

Thermochemical processes are promising systems for heat storage purpose. Such storage systems involve a reversible chemical reaction between a solid and a gas and one of their development challenge is the choice of the reactive pair. This pair has to fulfill a number of criteria, especially good thermodynamic properties, a good stability, low cost... Nevertheless, at present no reactive material fulfills all of these criteria. However, it can be interesting to combine several reactive pairs in order to take advantage of their respective qualities.

This paper investigates the thermodynamic functioning of an open thermochemical reactor containing a fixed bed of several salts. To this end, the sharp front model has been extended to a multisalt thermochemical reactor. This analytical model is based on the hypothesis of reaction fronts moving in the reactive bed crossed by moist air. It allows studying the operating of multi-salts thermochemical reactors, highlighting the interest of such systems and evaluating their reaction times (and therefore the power supplied/received). As an illustration, the case of a reactive bed of two salts (SrBr₂/CaCl₂) has been studied. This multisalt bed allowed the air temperature increase up to six times compared to that obtained with a reactive bed of only CaCl₂.

Keywords:

Open thermochemical system, multisalt, thermodynamic analysis, multisalt sharp fronts model

1. Introduction

Thermochemical processes are promising systems for thermal storage purposes [1]. Such systems have numerous advantages, especially a high storage density : around 200 to 500 kWh.m⁻³; as a matter of comparison, the energy density is about 90 kWh.m⁻³ for latent storage and about 54 kWh.m⁻³ for sensible heat storage (water, ΔT= 70 °C, 25% heat losses [2]). They also present negligible heat losses between the storage and release periods (the energy is stored as a chemical potential). Furthermore, these systems can cover a wide range of power (W/m³ to several kW/m³) and temperatures (30 to >500°C), allowing their use in many applications (house heating (2-4 kW, 30-60°C) [3,4], district heating (kW-MW, 60-180°C) [5], CSP (kW-MW, >300°C) [6], ...).

Solid/gas thermochemical systems involve a reversible monovariant chemical reaction between a porous solid and a reactive gas:



The synthesis of the solid ($A \rightarrow B$) is exothermic (heat recovery/discharge period), while its decomposition ($A \leftarrow B$) requires a heat input (storage/charging period). The equilibrium conditions (p_{eqSG} , T_{eqSG}) of such solid/gas reactions follow the Clausius–Clapeyron relation:

$$\ln \left(\frac{p_{eqSG}}{p^0} \right) = - \frac{\Delta h_r^0}{R T_{eqSG}} + \frac{\Delta s_r^0}{R} \quad (2)$$

Where p^0 is the reference pressure (1 bar). Thus, the thermodynamic equilibrium conditions can be determined using only one intensive variable: the equilibrium gas pressure p_{eqSG} or the equilibrium temperature of the bed T_{eqSG} .

Thermochemical systems using a hydrate/water pair can operate in two different modes: the closed and the open mode. In a closed thermochemical reactor, the salt reacts with pure water vapour (usually at low pressure), while in an open system the reactive solid bed is crossed by a moist air flow, at atmospheric pressure. For this specific case, the thermodynamic equilibrium conditions are related to the partial pressure of water in moist air.

One of the key points of thermochemical systems is the choice of the reactive pair. This pair has to fulfill a number of criteria, especially a high energy density, a low environmental impact, good thermodynamic properties (low (high) charge (discharge) temperature), a good stability and a low cost. Numerous reactive pairs have been proposed in the literature. Nevertheless, up to now, no reactive material fulfills all of these criteria [7,8]. Thus, it can be interesting to combine several reactive pairs in order to take advantage of their respective properties. For example, an expensive salt with good thermodynamic properties could be combined with a cheaper salt with less interesting thermodynamic properties.

The operating principle of thermochemical processes using multisalt reactors has already been studied for systems operating in a closed mode [9,10]. Promising results have been obtained. Especially, such processes allow using a wide range of charging temperatures and they have different operating temperatures for a given same working pressure. Nevertheless, no study deals with the functioning principle of thermochemical multisalt reactors operating in an open mode.

This paper focuses on the analysis of the thermodynamic functioning of an open thermochemical reactor using a packed bed containing several salts. Thus, the heat and mass transfers in such systems are investigated. To this end, from thermodynamic considerations of open thermochemical systems, the sharp front model, validated in a previous work for open thermochemical systems using a packed bed of one salt, is extended to multisalt thermochemical reactors. This analytical model is based on the Darcy's equation in a porous reactive bed crossed by moist air and the hypothesis of reaction fronts moving in the reactive bed. It allows to study theoretical cases of multisalt thermochemical reactors and to highlight the operating and the interest of such systems.

2. Open thermochemical storage system: functioning analysis

An open thermochemical heat storage system works with moist air and includes a solid/gas reactor containing a porous fixed bed of reactive solid. In such system, the reactive media is crossed by moist air. Thus, during the hydration (dehydration) phase, cold (hot) and humid air at T_i and p_{vi} (input conditions) is supplied to the system. The exothermic (endothermic) reaction leads to an increase (decrease) of the air temperature and to a decrease (increase) of the air humidity. Thus, the system rejects hot (colder) and less humid (more humid) air at T_j and p_{vj} (output conditions).

The operating principle of such system using a fixed bed reactor of one or several salts is presented in this section.

2.1. The sharp front model

A model of transformation of an open thermochemical fixed bed reactor containing one salt has already been applied and validated in a previous work [11]. This model allows estimating the reaction time of the salt during hydration or dehydration. Only the most important aspects of this model are presented below.

The main assumption of this 1D analytical model is the existence of a sharp front where the thermochemical reaction takes place. Indeed, an open thermochemical storage system using a fixed bed requires a high bed density and large quantities of non-reactive fluid (dry air) passing through

it. Thus, in such systems, the mass transfer is usually the main limitation of the reaction [12]. Heat transfer and kinetic limitations can therefore be neglected. In consequence, this working mode leads to a reaction front moving axially along the bed, according to gas diffusion in it. The reactive bed is then separated into two layers, one hydrated and the second dehydrated (see Figure 1).

In such reactive bed, the reaction front position, Z_f , can be directly related to the bed thickness Z_s and the reaction advancement X as: $Z_f = (1 - X)Z_s$ in hydration and $Z_f = XZ_s$ in dehydration.

Furthermore, neglecting kinetic limitations implies that the reaction front is at the thermodynamic equilibrium.

Additional simplifying assumptions are used:

- a) mass transfer is unidirectional
- b) there is no accumulation of heat or gas in the porous volume
- c) the transformation of the reactant is quasi-static (between the reaction advancement X and $X + dX$, all physical quantities are constant)
- d) moist air is considered as an ideal gas
- e) the air front conditions (p_{vf} and T_f) correspond to the output air conditions (p_{vj} and T_j).

Thus, for a constant air flow crossing the reactive bed and knowing the input air conditions, it is possible to determine the time needed to achieve a given reaction advancement X :

$$t_X = X \frac{v_S m_S M_h}{\dot{m}_{hi} M_S \left(1 - \frac{\left(1 - \frac{p_{vi}}{p_t}\right)}{\left(1 - \frac{p_{vf}}{p_t}\right)} \right)} \text{ in hydration case} \quad (3)$$

$$\text{and } t_X = (1 - X) \frac{v_S m_S M_h}{\dot{m}_{hi} M_S \left(1 - \frac{\left(1 - \frac{p_{vi}}{p_t}\right)}{\left(1 - \frac{p_{vf}}{p_t}\right)} \right)} \text{ in dehydration case.} \quad (4)$$

The moist air conditions at the reaction front (p_{vf} and T_f) are determined using the charge/discharge operating line. Indeed, from energy balances on the moist air and the reactive bed, assuming stationary operation and neglecting heat losses, previous works [13,14] have defined and validated a simple linear relationship between the input and output air conditions (T_i , p_{vi} , T_j , p_{vj}) of an open thermochemical fixed bed during reaction:

$$T_j(w_j) = \frac{\Delta h_r^0}{(c_{ma} + w_i c_{mv}) v M_v} (w_i - w_j) + T_j \quad (5)$$

Thus, according to the monovariance of the equilibrium and assuming that the reaction front is at thermodynamic equilibrium, it is possible to define the moist air conditions at the reaction front. These correspond to the intersection between the equilibrium line of the reaction (defined by Eq. (2)) and the charge/discharge operating line (defined by Eq. (5)). Thus, the output air conditions depend only on the characteristics of the solid/gas reactive pair and the input air conditions.

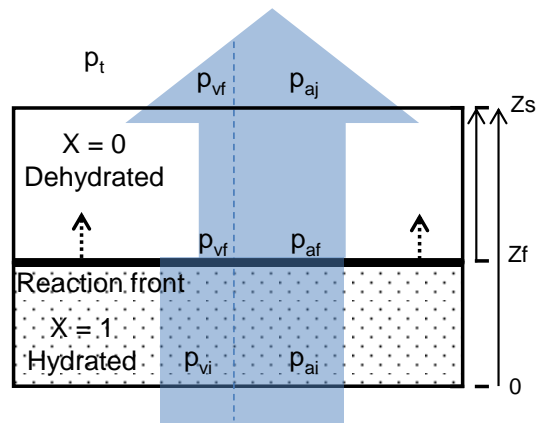


Figure 1: Schematic representation of a reactive bed crossed by a flow of moist air.

2.3 – Multisalt reactor modeling: the multisalt sharp fronts model

The thermodynamic functioning and modeling of an open thermochemical reactor containing several types of hydrate salts mixed in a homogenous fixed bed, is described and analyzed in this section. As the hydration and dehydration cases functioning are similar, only the hydration case is presented below. Furthermore, the functioning principle of such system can be easily extended to a reactor composed of a succession of reactive beds of one salt (cascade reactors).

2.3.1. Reaction fronts

Using the assumptions of the sharp front model (cf. §2.2), we can consider that in a multisalt reactive bed, each salt reacts along a sharp front moving axially through the bed. Thus, in a system using two reactive salts, two reactive fronts separate the bed into three layers: the first one where both salts are hydrated, the second one where one salt is hydrated and the other is dehydrated and the last one where both salts are dehydrated. Thus, for a system using “n” reactive salts, the reactive bed is separated into “n+1” layers. A schematic representation of the reactive bed of “n” salts (and “n” reaction fronts) is presented in Figure 2a.

Furthermore, in such system the charge/discharge operating line can be easily extrapolated. In this case, the air conditions at each reaction front (output air conditions) depend on the air conditions of the previous front (input air conditions). Thus, as shown in Figure 2b, the air conditions of each reaction front are coupled and the global output air conditions depend on the different types of salts used in the reactor. The knowledge of the front positions is therefore necessary to estimate the bed reaction rate and the system performances (power, temperature).

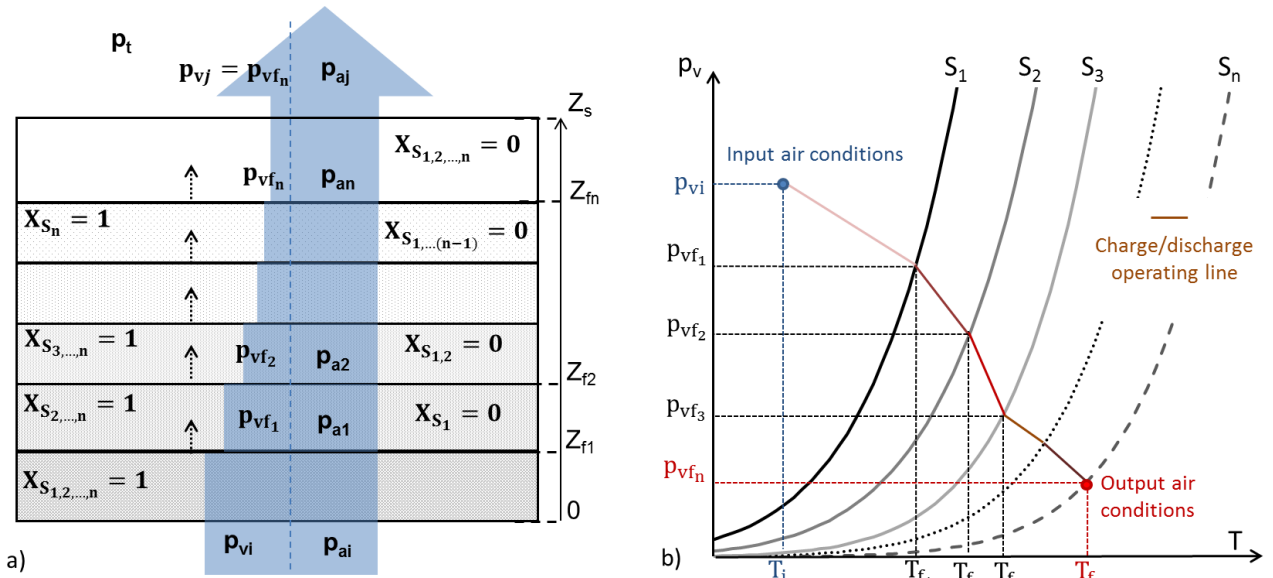


Figure 2: a) Schematic representation of the multisalt reactive bed, crossed by a flow of moist air during hydration. b) Equilibrium lines of the “n” reactive salts and their charge/discharge operating lines, represented in a Clapeyron diagram.

2.3.2. Fronts positions

At the beginning of the hydration phase, the reactive salts are all in their dehydrated state. Hydration conditions are imposed to the reactor, i.e. cold and humid air is supplied to the reactive bed. The salt with the biggest equilibrium drop (difference between the operating temperature and pressure and the equilibrium thermodynamic values, as the salt S_n , cf. Figure 2b), reacts first on a front which moves axially along the moist air flow direction and is at position Z_{fn} (Figure 2a). For $Z > Z_{fn}$, the air is at the thermodynamic equilibrium temperature and vapour pressure of the salt S_n , corresponding to dehydrated conditions for the other salts. Thus, the other salts can not react in this area. Afterward, the salts S_{n-1} , then S_{n-2}, \dots and S_1 , react each after the other on a sharp front.

Thus, the “n” reactive fronts are distributed in function of their thermodynamic equilibrium position. The reaction front of the leftmost salt on the Clapeyron diagram, is located the nearest to the air inlet. Follow, in order, the other reaction fronts until the rightmost salt in the Clapeyron diagram, which is located nearest to the air outlet (Figure 2a).

Inversely, in dehydration the reactive front of the salt S_1 is nearest to the air outlet and the S_n front is nearest to the air inlet.

From the knowledge of the reactive fronts order, it is then possible to evaluate the thermodynamic equilibrium at each front and to determine the output air conditions and the reaction time of each salt.

2.3.3. Reaction time of the multisalt bed

The sharp front model has shown that the reaction front evolution depends only on the characteristics of the solid/gas reactive pair and the input air conditions. Similarly, in a multisalt reactive bed, we consider that each reaction front behaves like a sharp front of a reactive bed of one salt. In this case, the reaction front evolution of each salt depends to the air conditions of the previous reaction front instead of the input air conditions. Therefore, although the reaction times of each salt are coupled, knowing the air conditions at each reaction front and the front orders in the bed (cf. §2.3.1 and §2.3.2), it is possible to define the reaction time of the salt S_k as:

$$t_{S_k} = X \frac{v_{S_k} m_{S_k} M_h}{\dot{m}_{hi} M_{S_k} \left(1 - \frac{\left(1 - \frac{p_{vf_{k-1}}}{p_t} \right)}{\left(1 - \frac{p_{vf_k}}{p_t} \right)} \right)} \quad (\text{hydration case}) \quad (6)$$

$$\text{and } t_{S_k} = (1 - X) \frac{v_{S_k} m_{S_k} M_h}{\dot{m}_{hi} M_{S_k} \left(1 - \frac{\left(1 - \frac{p_{vf_{k-1}}}{p_t} \right)}{\left(1 - \frac{p_{vf_k}}{p_t} \right)} \right)} \quad (\text{dehydration case}). \quad (7)$$

Furthermore, let's recall that the air conditions after crossing the reactive front of the salt S_k (at the thermodynamic equilibrium of the salt S_k) do not allow the reaction of the salt S_{k-1} . In such system, the reaction time of the salt S_{k-1} , and more generally of the salt S_{k-i} , is necessarily higher than or equal to the reaction time of the salt S_k . Thus, the reaction time of the salt S_{k-1} can be limited by the reaction time of salt S_k .

In this particular case, the salt S_{k-1} is crossed by most vapour that can react, and the thermodynamic equilibrium is not reached at the S_{k-1} front. The water partial pressure at this reaction front ($p_{vf_{k-1}}$) is calculated such that $t_{S_k} = t_{S_{k-1}}$. The front temperature T_{fk-1} is then deduced with the charge/discharge operating line.

In order to avoid that one reactive salt limits the others, and thus to use the properties of each reactive salt during all the reaction, it is necessary to correctly size the multisalt system. Especially, all reactive salts have to react until the end of the reaction in the multisalt bed. Thus, the optimal size of the reactive bed corresponds to the mass of each salt such as: $t_{S_1} = t_{S_k} = t_{S_n}$. Let:

$$\frac{v_{S_1} m_{S_1} M_h}{\dot{m}_{hi} M_{S_1} \left(1 - \frac{\left(1 - \frac{p_{vi}}{p_t} \right)}{\left(1 - \frac{p_{vf_1}}{p_t} \right)} \right)} = \frac{v_{S_k} m_{S_k} M_h}{\dot{m}_{hi} M_{S_k} \left(1 - \frac{\left(1 - \frac{p_{vf_{k-1}}}{p_t} \right)}{\left(1 - \frac{p_{vf_k}}{p_t} \right)} \right)} = \frac{v_{S_n} m_{S_n} M_h}{\dot{m}_{hi} M_{S_n} \left(1 - \frac{\left(1 - \frac{p_{vf_{n-1}}}{p_t} \right)}{\left(1 - \frac{p_{vf_n}}{p_t} \right)} \right)} \quad (8)$$

From this equation, we can deduce the following relation for the salt "k" and "l":

$$\frac{m_{S_k}}{m_{S_l}} = \frac{v_{S_l} M_{S_k} \left(1 - \frac{\left(1 - \frac{p_{vf_{k-1}}}{p_t} \right)}{\left(1 - \frac{p_{vf_k}}{p_t} \right)} \right)}{v_{S_k} M_{S_l} \left(1 - \frac{\left(1 - \frac{p_{vf_{l-1}}}{p_t} \right)}{\left(1 - \frac{p_{vf_l}}{p_t} \right)} \right)} \quad (9)$$

Note that $p_{vf_0} = p_{vi}$.

It is also possible to determine the optimal mass fraction of the salt "l" as:

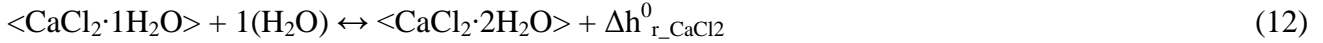
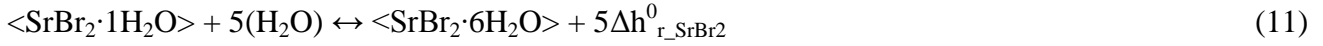
$$\frac{m_{S_l}}{m_{Tot}} = \frac{1}{\sum_k \frac{m_{S_k}}{m_{S_l}}} \quad (10)$$

Note that the optimal mass fraction of the salt "l" depends on the input air conditions, on its solid/gas reaction characteristics and on the characteristics of the others solid/gas reactions involved.

3. Case study: mix of CaCl₂ and SrBr₂

This case study presents the functioning of a multisalt reactive bed composed of a mix of two reactive hydrates: the SrBr₂/H₂O pair and the CaCl₂/H₂O pair. These two reactive pairs have been largely studied and seem promising for low temperature thermal storage applications [11,13,15].

The thermochemical reactions are:



Their standard enthalpy and entropy of reaction are: $\Delta h_{r,\text{SrBr}_2}^0 = 6400 \text{ J}\cdot\text{mol}^{-1}_v / \Delta s_r^0 = 175 \text{ J}\cdot\text{mol}^{-1}_v\cdot\text{K}^{-1}$ [16] and $\Delta h_{r,\text{CaCl}_2}^0 = 47000 \text{ J}\cdot\text{mol}^{-1}_v / \Delta s_r^0 = 104 \text{ J}\cdot\text{mol}^{-1}_v\cdot\text{K}^{-1}$ [17] respectively for the SrBr₂/H₂O pair and the CaCl₂/H₂O pair.

The functioning and the design of this multisalt reactive bed are presented in this section, for the hydration phase.

3.1 – Functioning and parametric study

The operating and equilibrium conditions of the two reactive pairs are presented in the Clapeyron diagram in Figure 3. Thus, for input air conditions of 20°C and 1500 Pa (realistic input conditions for a storage system for house heating application), and using the multisalt sharp fronts model, the output air temperature can be calculated. A temperature of 44.4°C ($T_{j,\text{Mix}}$) is obtained.

Compared to the output air temperature of a reactive bed of one salt of SrBr₂ or CaCl₂ (respectively 38.4°C (T_{f,SrBr_2}) and 41.3°C (T_{j,CaCl_2})), the multisalt bed thus allows to increase this latter at least of 3.1°C, for the studied case.

In general, the output air temperature difference between the multisalt reactive bed and the bed of the rightmost reactive salt in the Clapeyron diagram (CaCl₂ in the case study: $\Delta T = T_{j,\text{Mix}} - T_{j,\text{CaCl}_2}$), depends only on the characteristics of the solid/gas reactions and the input air conditions.

A parametric study of the influence of the input air conditions (in the range of 0-40°C and 500-2500 Pa) on the temperature difference is presented in Figure 4 for the SrBr₂/CaCl₂ multisalt bed. The maximum temperature difference is for the lowest inlet temperature and the highest inlet water partial pressure. Which means that ΔT of 6.8°C is obtained for $T_i = 0^\circ\text{C}$ and $p_{vi} = 2500 \text{ Pa}$. Inversely, the lowest temperature difference is obtained for the highest inlet temperature and lowest water partial pressure. In this case the ΔT is null. This corresponds to input air conditions that do not allow the hydration of the SrBr₂/H₂O reactive pair. Therefore, it is important to know the input air conditions of the open thermochemical system in order to evaluate its performances.

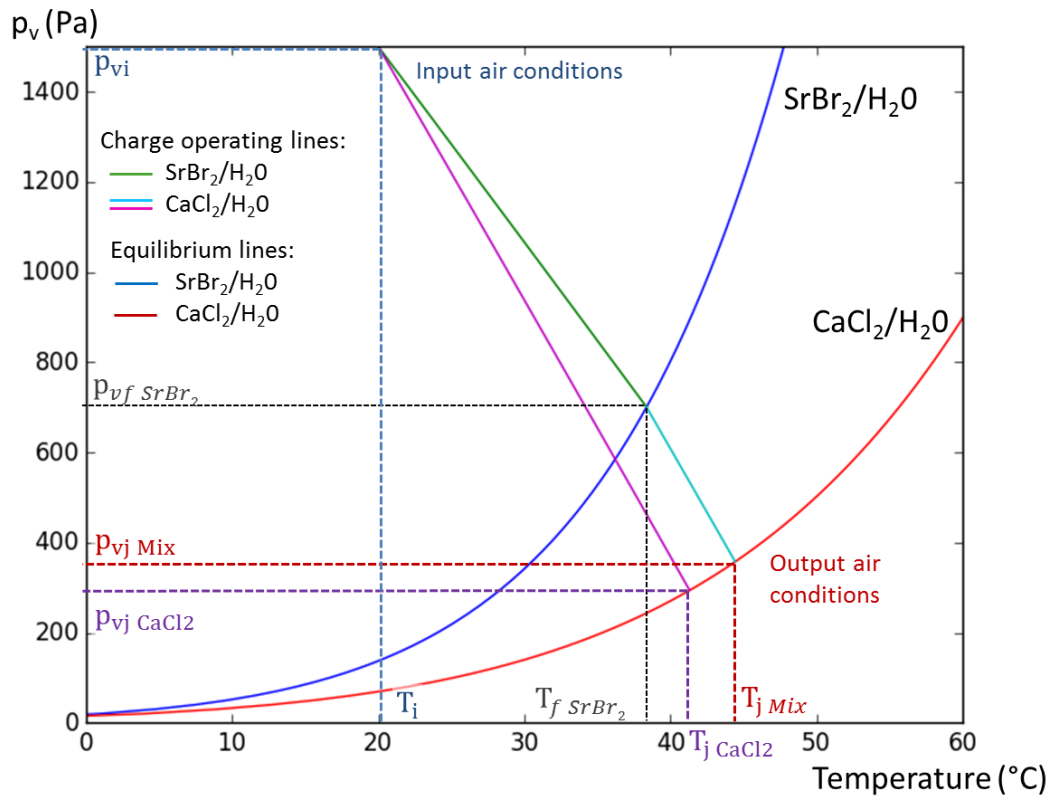


Figure 3: Equilibrium lines and charge operating lines of the solid/gas reactions ($\text{SrBr}_2/1-6\text{H}_2\text{O}$) and ($\text{CaCl}_2/1-2\text{H}_2\text{O}$).

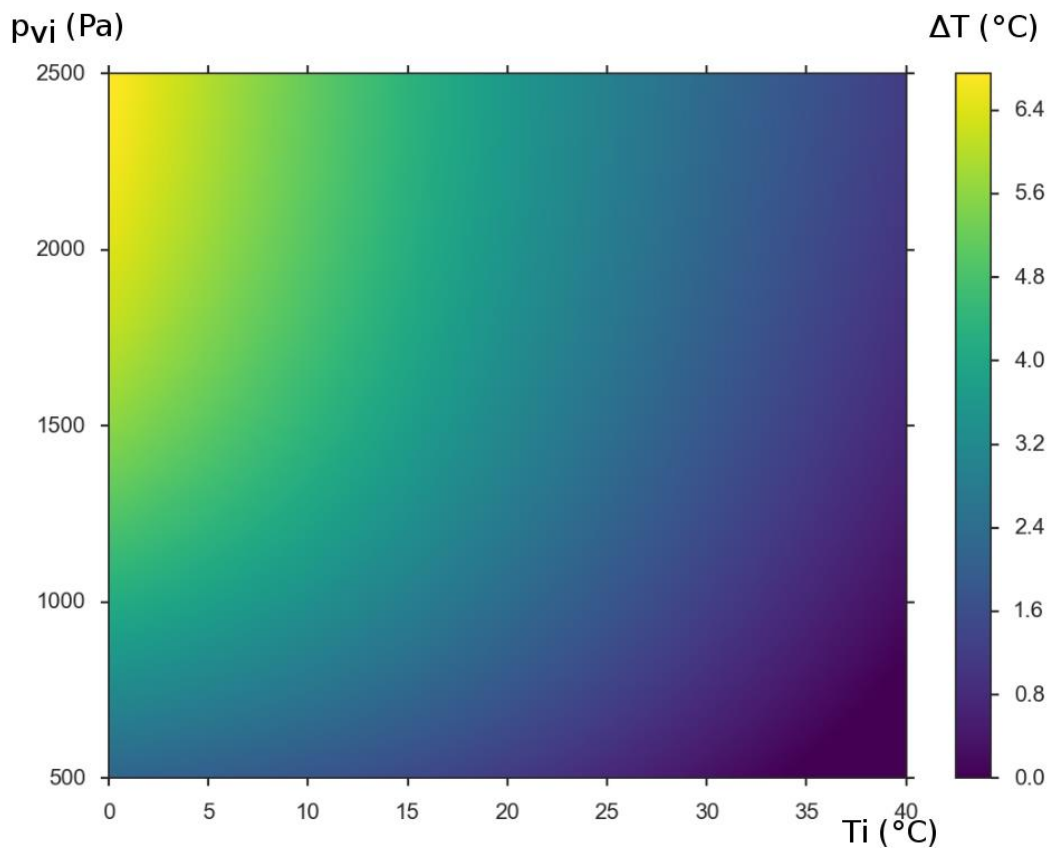


Figure 4: Map of the influence of the input air conditions (T_i , p_{vi}) on the output air temperature difference between the multisalt reactive bed and the bed of CaCl_2 ($\Delta T = T_{j, \text{Mix}} - T_{j, \text{CaCl}_2}$).

3.2 – Optimal salts masses

As shown in §2.3.3, in order to avoid that one reactive salt limits the others, it is necessary to correctly size the mass fraction of each reactive salt of the multisalt bed. Let's recall that this optimal mass fraction depends of the reactive pairs characteristics and the air input conditions (see Eq. 10).

A color map of the optimal mass fraction of SrBr_2 in the multisalt reactive bed as function of the input air conditions is presented in the Figure 5. The optimal mass fraction of SrBr_2 varies widely with the input air conditions. Thus, in the studied range (0-40°C for the input air temperature and 500-2500 Pa for the input water partial pressure), the optimal mass fraction changes between 0 and 0.9. As an example, for the input air condition of 20°C and 1500 Pa, the optimal mass fraction of SrBr_2 is 0.52.

The mass fraction of SrBr_2 is high for low input air temperatures and water partial pressures. On the contrary, for high temperatures and low water partial pressures, the optimal mass fraction of SrBr_2 is low. Note that the side where the mass fraction is equal to 0 corresponds to air conditions not allowing the $\text{SrBr}_2/\text{H}_2\text{O}$ reaction.

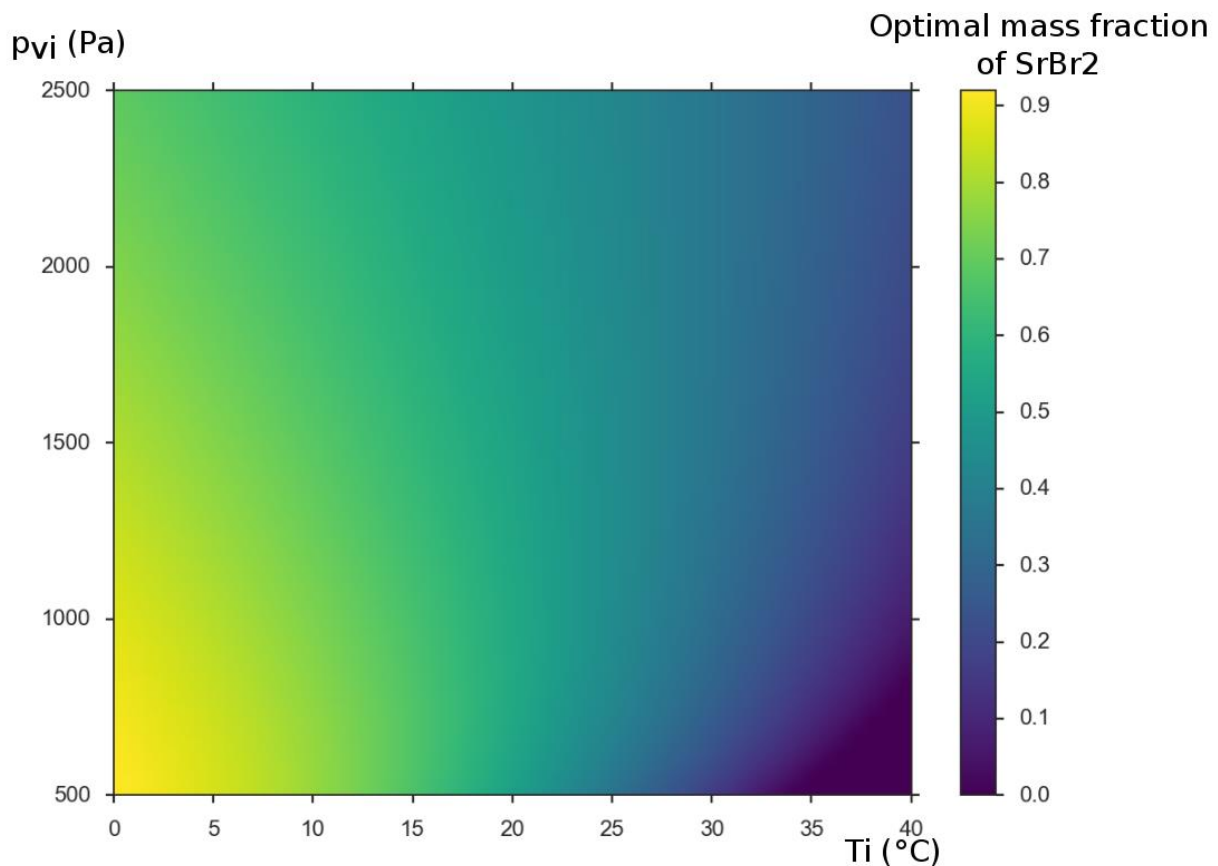


Figure 5: Map of the influence of the input air conditions (T_i , p_{vi}) on the optimal mass fraction of SrBr_2 in the reactive bed of two salts (SrBr_2 , CaCl_2).

4. Conclusion

This work investigates the operating principle of an open thermochemical storage containing a multisalt reactive bed. This paper focuses on the reactive bed transformation and thermodynamic analysis during hydration/dehydration reactions.

First, using the assumption of sharp reaction fronts moving axially along the moist air flow in the bed, the operating principle of such system has been studied. Furthermore, a simplified model has

been developed. This model allows estimating the reaction time and the power supplied/received by the reactive bed as function of the input air conditions and the characteristics of the solid/gas reactions. This model also allows to determinate the optimal mass fraction of each reactive salt in the multisalt bed.

Using this model, a case study of a reactive bed of two salts ($\text{CaCl}_2/\text{SrBr}_2$) has been investigated during the hydration phase. This study has shown that using a multisalt reactive bed could increase the performances of the storage system. Indeed, the $\text{CaCl}_2/\text{SrBr}_2$ multisalt bed allowed increasing the output air temperature (and therefore the power supplied) up to six degree compared to that obtained with a reactive bed of only CaCl_2 . Furthermore, the optimal mass fraction of each reactive salt has been determined. Finally, we observed that the system output air temperature and the optimal mass fractions strongly change with the input air conditions.

Thus, the open thermochemical reactors containing a multisalt reactive bed are promising systems for heat storage applications. Furthermore, the multisalt sharp front model is a simple tool allowing the pre-design of such systems.

Nomenclature

A	dehydrated reactive solid
B	hydrated reactive solid
S	Reactive salt
\dot{m}	mass flow rate, $\text{kg}\cdot\text{s}^{-1}$
m	masse, kg
M	molar mass, $\text{kg}\cdot\text{mol}^{-1}$
p	pressure, Pa
R	gas constant, $\text{J}\cdot\text{mol}^{-1}\cdot\text{K}^{-1}$
T	temperature, K
T'	temperature, °C
t	reaction time, s
w	mass water content, kg_v/kg_a
X	reaction advancement
Z_f	reaction front position, m
Z_s	reactive bed thickness, m

Greek symbols

Δh_r^0	standard enthalpy of reaction, $\text{J}\cdot\text{mol}^{-1}_G$
Δs_r^0	standard entropy of reaction, $\text{J}\cdot\text{mol}^{-1}_G\cdot\text{K}^{-1}$
v	stoichiometric coefficient, $\text{mol}_G\cdot\text{mol}_S^{-1}$

Subscripts

eqSG	solid / gas equilibrium
f	at the reaction front
G	gas
h	moist air
i	inlet of the porous bed
j	outlet of the porous bed
k	k^{th} reactive salt
l	l^{th} reactive salt
n	n^{th} reactive salt

S salt
t total
v water vapor
X reaction advancement

Superscripts

0 reference

References

- [1] Aydin D, Casey SP, Riffat S. The latest advancements on thermochemical heat storage systems. *Renew Sustain Energy Rev* 2015;41:356–67. doi:10.1016/j.rser.2014.08.054.
- [2] Hadorn J-C. Advanced storage concepts for active solar energy—IEA SHC Task 32 2003-2007. *Proceeding Eurosun, Lisbon, Portugal*: 2008.
- [3] N'Tsoukpoe KE, Liu H, Le Pierrès N, Luo L. A review on long-term sorption solar energy storage. *Renew Sustain Energy Rev* 2009;13:2385–96. doi:10.1016/j.rser.2009.05.008.
- [4] Pinel P, Cruickshank CA, Beausoleil-Morrison I, Wills A. A review of available methods for seasonal storage of solar thermal energy in residential applications. *Renew Sustain Energy Rev* 2011;15:3341–59. doi:10.1016/j.rser.2011.04.013.
- [5] Farcot L, Le Pierrès N, Papillon P. Etude et analyse d'un stockage thermochimique avec réacteur séparé adapté à des températures comprises entre 60°C et 120°C. *Journ. Natl. L'Énergie Sol., Perpignan (France)*: 2015.
- [6] Prieto C, Cooper P, Fernández AI, Cabeza LF. Review of technology: Thermochemical energy storage for concentrated solar power plants. *Renew Sustain Energy Rev* 2016;60:909–29. doi:10.1016/j.rser.2015.12.364.
- [7] Tatsidjodoung P, Le Pierrès N, Luo L. A review of potential materials for thermal energy storage in building applications. *Renew Sustain Energy Rev* 2013;18:327–49. doi:10.1016/j.rser.2012.10.025.
- [8] Trausel F, de Jong A-J, Cuypers R. A Review on the Properties of Salt Hydrates for Thermochemical Storage. *Energy Procedia* 2014;48:447–52. doi:10.1016/j.egypro.2014.02.053.
- [9] Istria S, Castaing-Lasvignottes J, Neveu P. Energetic analysis, application field and performance of a new thermochemical sorption cycle: The multisalt system. *Appl Therm Eng* 1996;16:875–89. doi:10.1016/1359-4311(96)00007-5.
- [10] Li TX, Wu S, Yan T, Xu JX, Wang RZ. A novel solid–gas thermochemical multilevel sorption thermal battery for cascaded solar thermal energy storage. *Appl Energy* 2016;161:1–10. doi:10.1016/j.apenergy.2015.09.084.
- [11] Michel B, Mazet N, Mauran S, Stitou D, Xu J. Thermochemical process for seasonal storage of solar energy: Characterization and modeling of a high density reactive bed. *Energy* 2012;47:553–63. doi:10.1016/j.energy.2012.09.029.
- [12] Michel B, Neveu P, Mazet N. Comparison of closed and open thermochemical processes, for long-term thermal energy storage applications. *Energy* 2014;72:702–16. doi:10.1016/j.energy.2014.05.097.
- [13] Marias F, Neveu P, Tanguy G, Papillon P. Thermodynamic analysis and experimental study of solid/gas reactor operating in open mode. *Energy* 2014. doi:10.1016/j.energy.2014.01.101.
- [14] Michel B, Mazet N, Neveu P. Experimental investigation of an innovative thermochemical process operating with a hydrate salt and moist air for thermal storage of solar energy: Global performance. *Appl Energy* 2014;129:177–86. doi:10.1016/j.apenergy.2014.04.073.
- [15] Zondag HA, Van Essen M, Bleijendaal L, Cot J, Schuitema R, Planje W, et al. Comparison of reactor concepts for thermochemical storage of solar heat. *Proceeding IRES, 2008*.
- [16] Mauran S, Lahmidi H, Goetz V. 3rd Intermediate Report, European project no NNE5-2000-00385. 2002.

- [17] Van de Voort IM. Characterization of a thermochemical storage material. Eindh Univ Technol Master Thesis 2007.